Journal of Power Sources 235 (2013) 87–94

Contents lists available at SciVerse ScienceDirect

Journal of Power Sources

journal homepage: www.elsevier.com/locate/jpowsour

Identifying lithium–air battery discharge products through ^{6}Li solid-state MAS and ^{1}H–^{13}C solution NMR spectroscopy

Laura A. Huff, Jennifer L. Rapp, Lingyang Zhu, Andrew A. Gewirth*

Department of Chemistry, University of Illinois at Urbana-Champaign, 600 S. Mathews Avenue, Urbana, IL 61801, USA

HIGHLIGHTS

- ^{6}Li, ^{13}C, and ^{1}H NMR spectroscopy is used to interrogate discharged lithium–O_2 battery cathodes.
- ^{6}Li NMR shows Li_2O_2 is the primary product from batteries with TEGDME solvent.
- Degradation products include lithium formate, lithium acetate, and lithium carbonate.

ARTICLE INFO

Article history:
Received 15 December 2012
Received in revised form
23 January 2013
Accepted 28 January 2013
Available online 6 February 2013

Keywords:
Li
Air
Battery
NMR

ABSTRACT

Discharged lithium–O_2 battery cathodes are investigated with different catalysts present including Pd, α-MnO_2 and CuO, and containing two different electrolyte solvents, 1:1 ethylene carbonate/dimethyl carbonate (EC/DMC) and tetraethylene glycol dimethyl ether (TEGDME). Solid-state ^{6}Li magic angle spinning (MAS) NMR spectroscopy has been used identify lithium products that are formed in the cathodes and differences between products formed with the different catalysts and solvents. There are significant differences in the products formed in Li–O_2 cathodes with the two different solvents, EC/DMC and TEGDME. Due to the small chemical shift range of lithium it is difficult to determine exact speciation from ^{6}Li MAS NMR data alone. Fitting of the ^{6}Li NMR peaks with tested Li-oxide powder standards indicates that Li–O_2 cathodes discharged in EC/DMC produce primarily Li_2CO_3 as a lithium product and those discharged in TEGDME produce mainly Li_2O_2. Solution 2D correlation ^{1}H–^{13}C NMR spectroscopy techniques allow for determination of side-products produced in Li–O_2 cathodes.

1. Introduction

The non-aqueous lithium–air battery or Li–O_2 battery, first reported in 1996 [1], has been the focus of considerable attention because its putative specific energy (3505 W h kg^{-1} [2]) is substantially larger than that found for Li-ion batteries and approaches the theoretical specific energy for gasoline/air engines (11,860 W h kg^{-1}). In Li-ion batteries the specific energy is limited by the positive electrode (150 mA h g^{-1} or a theoretical specific energy of 387 W h kg^{-1}) [3], which is itself the subject of substantial attention. The gravimetric capacity of the Li–air battery comes at the expense of volumetric capacity, where the Li–air battery is only slightly better than Li-ion (3436 W h L^{-1} for Li–O_2 vs. 1015 W h L^{-1} for Li-ion). The low volumetric energy density of Li–O_2 batteries arises from the need to store excess Li in the anode, since Li metal has a relatively low density (0.534 g cm^{-3}) [2].

The discharge reaction for the Li–O_2 battery involves the two-electron reduction of O_2, which migrates into a porous carbon (nanoporous gold catalyst has also been used as a cathode material) [4] cathode, and reacts with Li^+ ions from the lithium metal anode to produce lithium oxide products. The desired product is lithium peroxide, Li_2O_2, which is a theoretically reversible product with a reaction formal potential of 2.96 V, shown in Scheme 1 [5,6].

Several studies indicate that Li_2O_2 is the major discharge product formed in Li–O_2 battery cathodes [1,11,12]. Although Li_2O_2 is the full oxygen reduction product and forms preferentially, Li_2O (as depicted in Scheme 1, with E_{rev} = 2.91 V_{Li}), is the more desirable product because of its higher specific energy and energy density [5]. Li_2O formation has been suggested to occur by two different mechanisms, as shown in Scheme 1 with E_{rev} = 2.91 and 2.87 V_{Li}. However, recharge of a battery with a Li_2O product is problematic [13,14].

While Li–air batteries are in concept advantageous, several studies indicate that the carbonate solvents commonly used in these batteries decompose readily in Li–O_2 discharge systems to form Li_2CO_3 [15–17]. The search for a more robust solvent and

* Corresponding author. Tel.: +1 217 333 8329; fax: +1 217 244 5186.
E-mail address: agewirth@illinois.edu (A.A. Gewirth).

0378-7753/$ – see front matter © 2013 Elsevier B.V. All rights reserved.
http://dx.doi.org/10.1016/j.jpowsour.2013.01.158

$$2Li^+ + 2e^- + O_2 \leftrightarrow (Li_2O_2)_{solid} \quad E_{rev} = 2.96\,V$$
$$4Li^+ + 4e^- + O_2 \leftrightarrow 2(Li_2O)_{solid} \quad E_{rev} = 2.91\,V$$
$$(Li_2O_2)_{solid} + 2Li^+ + 2e^- \leftrightarrow 2(Li_2O)_{solid} \quad E_{rev} = 2.87\,V$$

Scheme 1. Reaction mechanisms for theoretical reactions that occur during Li–O_2 battery discharge at the cathode where E_{rev} is referenced vs. Li/Li^+ (as are all potentials throughout this study) [5–10].

electrolyte has led to a recent report suggesting that tetraethylene glycol dimethyl ether (TEGDME) and lithium triflate ($LiCF_3SO_3$) might result in a more robust battery exhibiting greater cyclability [18]. However, other studies suggest that ethers (such as DME, diglyme, triglyme, TEGDME and 1,3-dioxolane) [2] decompose during discharge to some extent as well, especially over the period of many cycles [19,20]. Thus, one large area of active study is to find a suitable electrolyte (i.e. salt + solvent system) that does not decompose or react with Li–O_2 products during cycling.

Another area seeing attention examines possible catalysts to reduce the overpotentials found during both discharge and recharge in Li–O_2 batteries. Noble metals such as Au and Pt [8,21] as well as a Fe/N/C composite [22] and mixed oxides such as MnO_2, bismuth and lead ruthenium oxides (pyrochlore oxides), spinel-based metal oxides on graphene (containing Ni, Co or Mn) and non-crystalline metal oxides on graphene [23–31] have been suggested as possible components of Li–O_2 cathodes. In order to design more effective catalysts, electrolyte systems (i.e. the Li salt and solvent) and cathode materials, there must be a method in place to identify the discharge products that are formed so that the discharge/charge chemistry may be well-understood and the system may be optimized for Li_2O_2 production.

NMR spectroscopy is extremely useful for the identification and structural determination of a wide variety of materials. Solid-state MAS NMR spectroscopy involves spinning the sample at an angle, θ_m (54.7°) with respect to the static magnetic field in order to mimic the free rotations of molecules in solution [32]. This orientation averaging reduces the three main interactions (dipolar, chemical shift anisotropy and quadrupolar), which can lead to extensive broadening of NMR lines that would otherwise dominate the spectra, resulting in little or no information to be obtained. Thus, MAS allows for well-resolved spectra of solid-phase materials [32,33].

Lithium has two stable NMR-active isotopes, ^7Li and ^6Li, both of which are quadrupolar nuclei (spin $I > ½$), with $I = 3/2$ and 1, respectively. ^7Li is approximately 93% naturally abundant, while ^6Li is only 7% naturally abundant. While the low natural abundance of ^6Li is a disadvantage for NMR studies, ^6Li has the advantage of a much smaller quadrupolar coupling constant (the smallest of all quadrupolar nuclei), providing spectra with narrow linewidths and high resolution in comparison with ^7Li spectra. The quadrupolar nature of the ^7Li nucleus complicates spectra and can cause line-splitting and asymmetric lineshapes [34]. Additionally, lithium generally has a small chemical shift range (ca. 2–5 ppm) [35,36], meaning that high resolution is important in order to obtain exact chemical shift information from Li NMR spectra. Therefore, the main advantage of ^6Li is that it behaves like a nucleus with $I = ½$, resulting in well-resolved spectra containing accurate chemical shifts.

In this paper, both ^6Li solid-state magic angle spinning (MAS) and $^1H/^{13}C$ solution-state NMR spectroscopy are used to identify and structurally characterize the discharge products of Li–O_2 carbon cathodes. There are a number of reports using NMR to examine Li–O_2 discharge products including ^6Li MAS NMR spectroscopy of cathodes containing ethylene carbonate/propylene carbonate (EC/PC) [37], ^7Li and ^{17}O NMR spectroscopy [38]. However, developments in both catalysts and solvent systems necessitate a more in-depth examination of discharge products using NMR. In particular, we report an in-depth study of two different solvent systems, a carbonate (1:1 ethylene carbonate/dimethyl carbonate, EC/DMC) and TEGDME as well as comparisons between several different cathode catalysts. In particular, we seek to understand whether discharge of a Li–O_2 battery in a non-carbonate solvent can yield a Li_2O_2 signal in the ^6Li MAS NMR and to identify putative decomposition products occurring during this process.

2. Experimental

Electrochemical measurements were performed using a modified [39]. Swagelok battery cell design (the Swagelok cell assembly is illustrated in Fig. S-1 in Supplementary data) [40]. The cell features stacked layers contained inside a Swagelok apparatus (nylon Swagelok tube fittings, ½″ inner diameter, purchased from Chicago Fluid System Technologies) consisting of a hollow aluminum cathode plunger and solid stainless steel anode plunger. The layers consisted of Li metal foil, a glass fiber separator (Whatman GF/F, 150 mm diameter), a carbon cathode with or without catalyst and a Ni mesh current collector. The carbon cathode was synthesized from a slurry containing carbon black (carbon Super C65, Timcal) 27 wt% + polyvinylidine fluoride (PVDF, Kynar 2801) 41 wt % + acetone (Sigma–Aldrich) + catalyst (if used) 32 wt%. For cathodes containing carbonate solvents (EC/DMC), propylene carbonate was added to the slurry, 61.9 wt%. The slurry was cast onto a glass surface, smoothed with a Gardco adjustable micrometer film applicator (Microm II, 5½″ width), and allowed to dry for ca. 5 min. The resulting cathode sheet was removed from the glass, and 1.2 cm diameter circles were punched out of the material. For all NMR experiments, the cathodes were first washed twice in acetonitrile for 10 min, and then dried under vacuum for 1 h.

Pd catalysts for the Li–O_2 cathodes were obtained from Fisher Scientific (specifications). α-MnO_2 was synthesized as described previously [24]. The electrolyte was 1 M $LiClO_4$ in 1:1 ethylene carbonate/dimethyl carbonate (EC/DMC, Sigma–Aldrich). The entire Swagelok apparatus was contained in a glass enclosure (illustrated in Figs. S-1 and S-2, Supplementary data) to allow for controlled O_2 flow. Cell assembly and disassembly were performed in an Ar-filled glove box (<0.5 ppm O_2). Samples for NMR were obtained by combining three cathodes into well-sealed 4 mm or 3.2 mm Si_3N_4 rotors.

Chronopotentiometry was performed using model 760C and 760D CHI instruments electrochemical workstations. Discharge current was 0.3 mA which was 150 mA g^{-1} on a whole cathode basis (i.e. battery discharge current and capacity was calculated per weight of the whole cathode). Discharge was continued until a cell voltage of 2.2 V was obtained. Lithium peroxide (95%), lithium oxide (97%), lithium carbonate (ACS reagent, ≥99.0%) and lithium hydroxide (reagent grade, ≥98%) powders were purchased from Sigma–Aldrich.

The $^{6,7}Li$ DPMAS and DPMAS Echo experiments were performed at both 7.1 T and 17.6 T on Varian Unity Inova 300 and Varian VNMRS 750 (Varian is now part of Agilent Technologies) spectrometers, respectively. The Varian Unity Inova 300 and Varian VNMRS 750 spectrometers were equipped with 4 mm Varian Chemagnetics APEX Double Resonance HX and Varian Narrow Bore Triple Resonance T3 MAS probes, respectively. The ^{13}C CPMAS spectra were acquired at 11.7 T on a Varian VNMRS 500 wide-bore spectrometer, equipped with a 3.2 mm Wide Bore Triple Resonance T3 Balun HCN probe. All samples were packed in silicon nitride rotors and spun at MAS rates of 10–15 kHz. $^{6,7}Li$ and ^{13}C chemical shifts were referenced to 1 M LiCl solution and TMS, respectively, at 0 ppm.

The experimental parameters for ^{6}Li MAS NMR are given in the figure captions, employing the following symbols: B_0 (magnetic field strength), ν_r (magic angle spinning rate), ν_{rf}^{X} (rf magnetic field applied to X spins), τ_{CP} (cross polarization time), $d1$ (relaxation delay) and NT (number of transients).

The ^{1}H–^{13}C one and two-dimensional solution NMR spectroscopy was performed on a Varian Inova 600 MHz spectrometer (14.1 T) equipped with a 5 mm triple-resonance HCN probe with Z-gradient capability and a 5 mm AutoX dual broadband probe with Z-gradient capability for direct ^{13}C detection. All experiments were recorded at 23 °C. All NMR samples were prepared via D_2O-extraction of cathode products in 5 mm NMR tubes after washing cathodes twice with acetonitrile. The ^{1}H and ^{13}C chemical shifts were referenced to tetramethylsilane (TMS) at 0 ppm [41].

The 2D TOCSY experiments reveal isolated continuously coupled spin systems in a molecule. The ^{1}H–^{13}C gHSQC (gradient Heteronuclear Single Quantum Coherence) data reveal one bond cross correlations between protons and carbons in a two dimensional format. The edited gradient-enhanced HSQC inverts the CH_2 signals, leaving those cross peaks negative and the CH and CH_3 cross peaks are positive (or vice versa). The ^{1}H–^{13}C gHMBC (gradient Heteronuclear Multiple Bond Correlation) data reveal the long-range bond correlations between proton and carbon nuclei from two to four bonds. These spectra provide crucial data for identification of molecular structures in solution [41].

The experimental parameters for ^{1}H and ^{1}H/^{13}C solution NMR are given in the figure captions, employing the following symbols: B_0 (magnetic field strength), sw (spectral window in the ^{1}H dimension), sw1 (spectral window in the ^{13}C dimension), pw (pulse width), pw90 (90° pulse width), $d1$ (relaxation delay), at (acquisition time), NT (number of transients) and ni (number of transients on the ^{13}C dimension).

3. Results

3.1. Discharge curves

Typical discharge curves obtained from Li–O_2 battery systems containing cathodes made using carbon only, carbon + α-MnO_2 (32 wt%), and carbon + Pd (32 wt%) are depicted in Fig. 1. Prior to discharge, the cell voltages were 2.9 ± 0.1 V for the carbon-only system, 3.0 ± 0.2 V for the carbon + Pd system, and 3.3 ± 0.1 V for the carbon + α-MnO_2 system. The discharge curves in Fig. 1 exhibit a sigmoidal shape, with the potential decreasing sharply upon initial discharge and then plateauing to a roughly steady discharge potential. Eventually, the cell potential drops sharply again until it reaches the cut-off potential of 2.2 V, which we used to mark the end of the discharge. This final potential was chosen as Li_2O_2 is said to be converted into Li_2O at potentials more negative than this value (Zhang, Read, J. Power Sources 195 (2010) 1235–1240).

3.2. Solid-state MAS ^{6}Li NMR of discharged cathodes

In order to obtain insight into speciation at the Li air battery cathode, ^{6}Li solid-state MAS NMR spectroscopy was employed to characterize discharged cathodes. Standards for comparison are provided by four lithium oxide powders implicated as possible Li–O_2 discharge products [5,6,17,19]. Spectra of the lithium oxide standard powders, collected at 17.6 T are shown in Fig. 2 (A table with the chemical shifts of discharged cathodes acquired at 7.1 T is provided in Supplementary data, showing similar chemical shifts, as expected.).

The four different Li oxide powders, depicted in Fig. 2, exhibit a range of different chemical shifts and linewidths. A previous study using ^{6}Li MAS NMR spectroscopy has been conducted on Li–O_2 cathodes containing ethylene carbonate/propylene carbonate (EC/PC) and the results shown in Fig. 2 agree well with the previously reported spectra [37]. We note that the chemical shift for

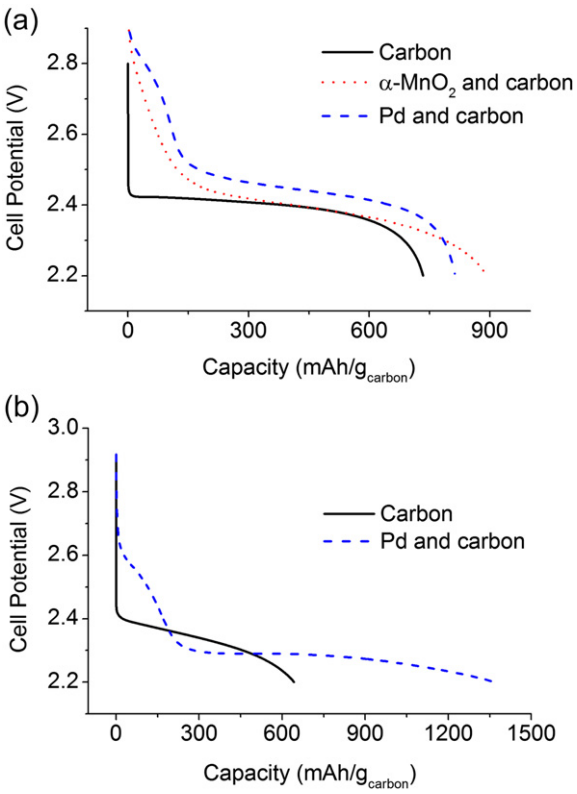

Fig. 1. Li–O_2 battery discharge curves for cathodes containing the different catalysts Pd, α-MnO_2 and carbon alone (a) at a discharge current of 0.3 mA (corresponding to ca. 157 mA $g^{-1}_{whole\ cathode}$) in 1 M $LiClO_4$ in EC/DMC and (b) at a discharge current of 140 mA g^{-1} in 0.3 M $LiClO_4$ in TEGDME.

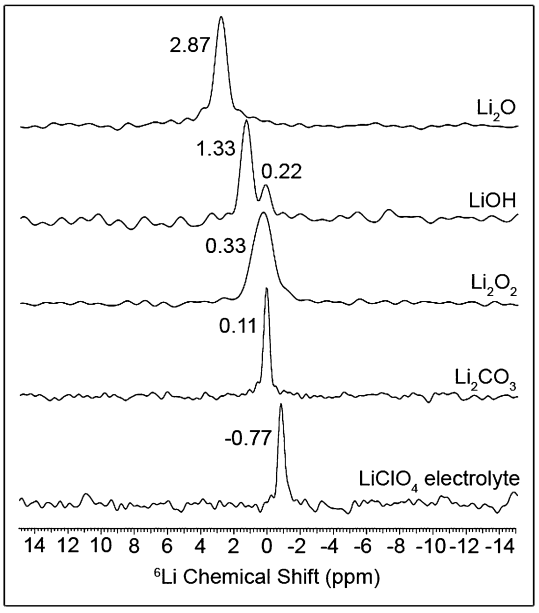

Fig. 2. ^{6}Li solid-state MAS NMR spectra of four lithium oxide powders and a solution of 1 M $LiClO_4$ in 1:1 EC/DMC (solution electrolyte used in Li–O_2 cells). B_0 = 17.6 T (750 MHz), ν_r = 12 kHz, $pw90_x$ = 2.5 μs, DP echo = 83 μs (echo was rotor synchronized), $d1$ = 600 s and NT = 32.

Li_2O_2 is slightly more positive than that reported previously [37] and attribute this to different sample preparations and conditions (i.e. extent of exposure to air).

Solid-state ^{6}Li MAS NMR spectra of discharged cathodes containing EC/DMC and 1 M $LiClO_4$ are shown in Fig. 3a after discharge to a cut-off potential of 2.2 V. Three different cathode catalyst materials were investigated: one consisting of Super C65 carbon-only + PVDF + PC and two others containing additional Pd or α-MnO_2.

The ^{6}Li NMR spectra obtained for the cathodes in EC/DMC (Fig. 3a) each consist of a single peak with chemical shifts ranging between −0.04 and 0.10 ppm. Table S-1 (in Supplementary data) provides chemical shifts and linewidths for all the samples examined here. These chemical shifts of cathodes in EC/DMC are grouped around the 0 ppm region, which is in contrast to the chemical shifts of cathodes containing TEGDME (Fig. 3b) that are grouped together in a region further downfield, ranging between 0.24 and 0.62 ppm (i.e. at more positive chemical shifts). The spectra of cathodes containing TEGDME (Fig. 3b) also each consist of a single peak that are centered around $\delta = 0.38$ ppm. Therefore, cathodes discharged in the two different solvents (EC/DMC and TEGDME) result in NMR chemical shifts that are grouped in two distinct regions and can thus be distinguished with ^{6}Li NMR spectroscopy.

3.3. Solution NMR from discharged cathodes

In order to investigate other discharge products that form upon decomposition of the two cathode solvents (i.e. by-products that form in addition to the dominant Li_2O_2 and Li_2CO_3 products), which has been reported previously [15,19] and contributes to the ^{6}Li NMR lineshapes (Fig. 3), solution ^{1}H/^{13}C NMR were collected from D_2O-extracted products formed in Li–O_2 cathodes. The different decomposition mechanisms that occur during discharge for each solvent system was realized and described previously [19], where it is suggested that by-product formation is initiated by combination of O_2 with electrons to form the superoxide radical, $O_2^{\cdot-}$. This superoxide radical then readily reacts with carbonate solvents (including EC, DMC and PC) [15] as well as ether solvents (DME, TEGDME, etc.) [19] to produce by-products through multiple-step radical reactions and polymerization reactions.

The ^{1}H NMR spectrum of products from carbon-only cathodes in EC/DMC is shown in Fig. 4, and the proposed structures elucidated using two-dimensional (2D) NMR are annotated on the figure. Several different types of 2D correlation NMR spectroscopy techniques were conducted to obtain structural information about the product compounds, including HSQC (Heteronuclear Single Quantum Coherence), HMBC (Heteronuclear Multiple Bond Correlation), COSY (COrrelation SpectroscopY) and TOCSY (Total COrrelation SpectroscopY) [41]. Representative 2D HMBC spectra for cathodes containing Pd and discharged in both EC/DMC and TEGDME are depicted in Fig. 5a and b. Only major products are evaluated here; minor products did not always yield cross-peaks that would confirm their identity.

4. Discussion

4.1. Discharge curves

The discharge curves obtained from Li–O_2 battery systems (including cathodes made using carbon only, carbon + α-MnO_2 (32 wt%), and carbon + Pd (32 wt%), depicted in Fig. 1), result in discharge voltage plateau values that are consistent with those previously reported for both carbon and α-MnO_2 cathodes, however they differ from the 2.96 V expected for a system where the open circuit potential is defined by the Li–Li_2O_2 couple [42]. In particular, the cell voltage of the carbon + α-MnO_2 cathodes at 3.3 V is too high to be associated with Li_2O_2 alone and has been attributed previously to a mixed potential from intercalation of Li^+ ions into the catalyst particles [11].

We next consider other possible half-cell reactions that might change the open circuit potential (OCP). Among many possible candidates, the formal potentials for Li_2O_2 and Li_2O most closely match the discharge potentials observed for Li–O_2 cathodes. Interestingly, several calculations conducted for different reactions that produce Li_2CO_3 yielded widely varying formal potentials, ranging from 0.09 to 5.87 V, as depicted in Table 1. It is therefore possible that the open circuit voltage of Li–O_2 batteries may arise from a combination of two or more of these various reactions rather

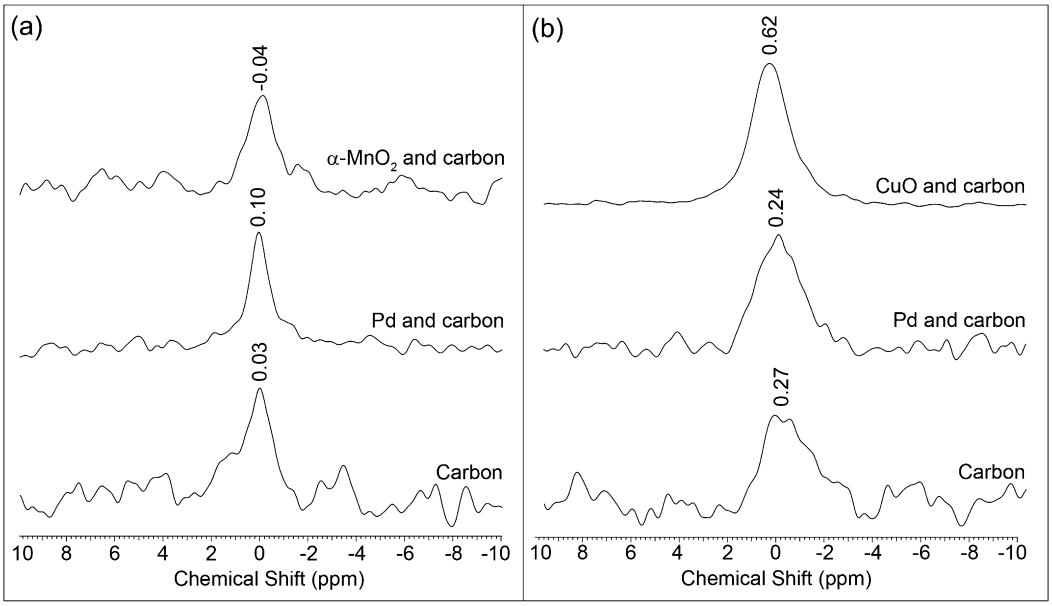

Fig. 3. ^{6}Li solid-state MAS NMR spectra of discharged Li–O_2 cathodes containing carbon, α-MnO_2 and Pd catalysts in (a) 1 M $LiClO_4$ in EC/DMC and (b) 0.3 M $LiClO_4$ in TEGDME. $B_0 = 17.6$ T (750 MHz), $\nu_r = 12$ kHz, $pw90_x = 2.5$ μs, DP echo = 83 μs(echo was rotor synchronized), $d1 = 300$ or 600 s and NT = 128–512.

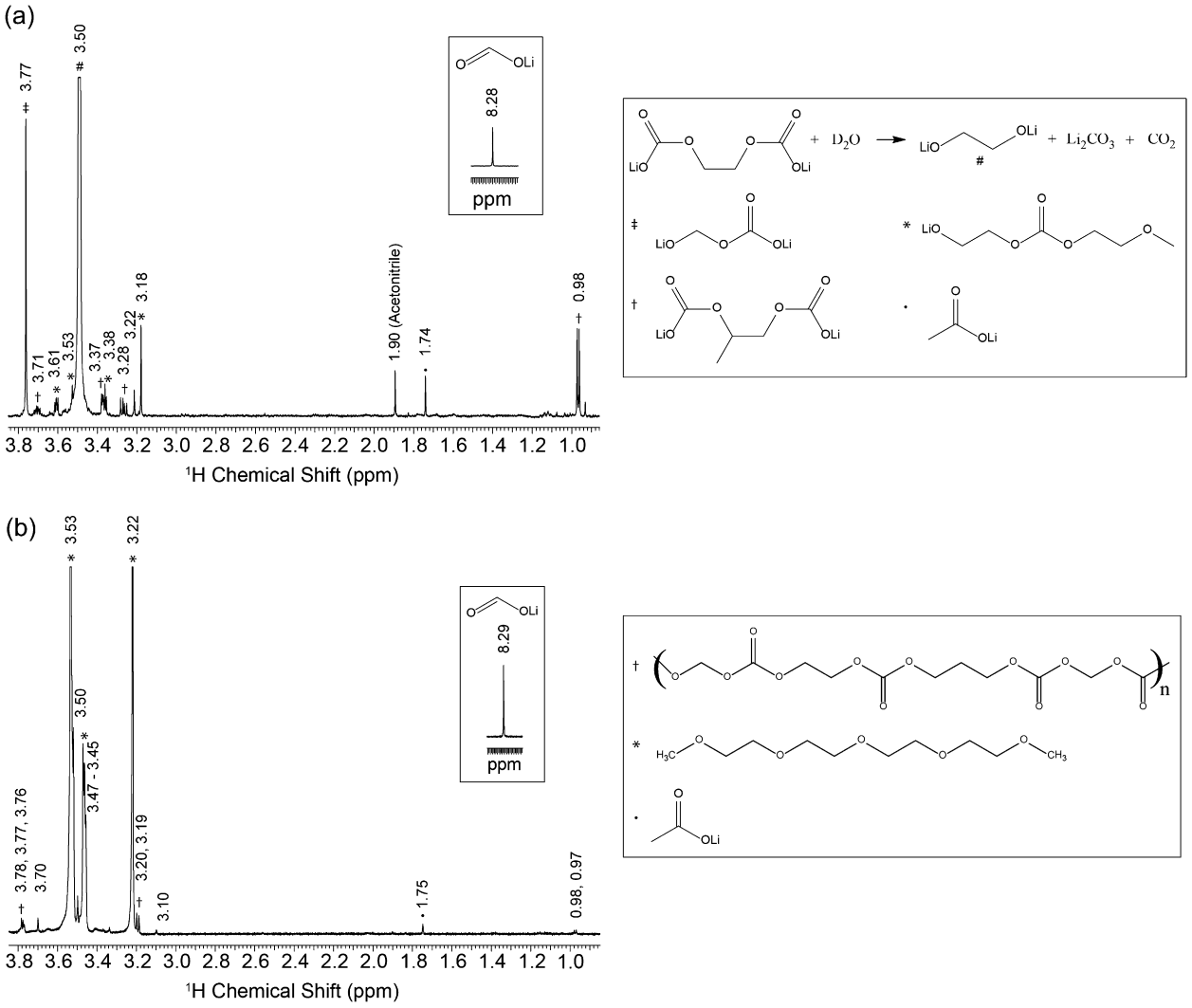

Fig. 4. ^{1}H solution NMR spectrum of products extracted from carbon-only cathodes containing (a) EC/DMC and (b) TEGDME in D_2O. Chemical shifts are depicted above each peak. The inset depicts the lithium acetate peak that is located farther downfield. The spectra were collected on a spectrometer with $B_0 = 14.1$ T (600 MHz), sw = 6134.5 Hz, for a 60° flip angle pw = 4 μs, at = 4 s, $d1 = 2$ s and NT = 32. The spectra were processed with zero-filling to 64k data points and a line-broadening of 0.5 Hz.

than from one reaction alone (i.e. a mixed potential), since the formal potentials of these reactions span the observed OCP values.

Interestingly, the shape of the discharge curves varied with the identity of the cathode catalyst. The cell voltage in the carbon-only system immediately drops to ca. 2.4 V, while the Pd system has a small shoulder at ca. 2.8 V before dropping after ca. 20% of discharge. The α-MnO_2-containing cathode exhibits behavior intermediate between these two cases.

The discharge curve exhibited in Fig. 1 also shows that cathodes containing different catalysts result in different discharge capacities. The discharge capacity $(\text{mA h g}^{-1}_{\text{whole cathode}})$ is determined from the start time of the discharge up to the time at which the 1.5 V set ending potential is reached. The mass of the whole cathode includes the carbon black, the binder and plasticizer, and the catalyst itself if present. The lowest capacity system was that containing carbon alone which exhibits a capacity of ca. 200 mA h $g^{-1}_{\text{whole cathode}}$. Although discharge capacities are known to be strongly dependent on the discharge rate [13,43] the capacities reported here are consistent with those reported previously on related systems [7]. Both the α-MnO_2 and Pd-containing cathodes yielded discharge capacities greater than that found for carbon alone, with increases in the order of 25%.

These results show that catalyst identity affects the discharge mechanism. The origin of this change could be one of several different causes including changes in reaction kinetics, pore structure of the cathode, identity of reaction intermediates and final products [11].

4.2. Solid-state MAS ^{6}Li NMR of discharged cathodes

^{6}Li solid-state MAS NMR spectroscopy of the four lithium oxide powders (tested as standards), depicted in Fig. 2, demonstrates that each of the standards displays a unique chemical shift value. The range in chemical shifts is due to the shielding effect, in which de-shielded nuclei shift downfield (to higher chemical shifts) and shielded nuclei shift upfield (to lower chemical shifts). For example, the Li nucleus in Li_2O is de-shielded by the electronegative oxygen atom and is therefore located further downfield than the Li peak from Li_2CO_3, which is de-shielded to a lesser extent by the carbonate group. The observation of two ^{6}Li peaks in the spectrum of LiOH is most likely due to the presence of both LiOH and the monohydrate form of LiOH ($LiOH \cdot H_2O$). Lithium hydroxide monohydrate, assigned to the peak at 0.22 ppm, is a compound known to form in the presence of water and has been shown previously to

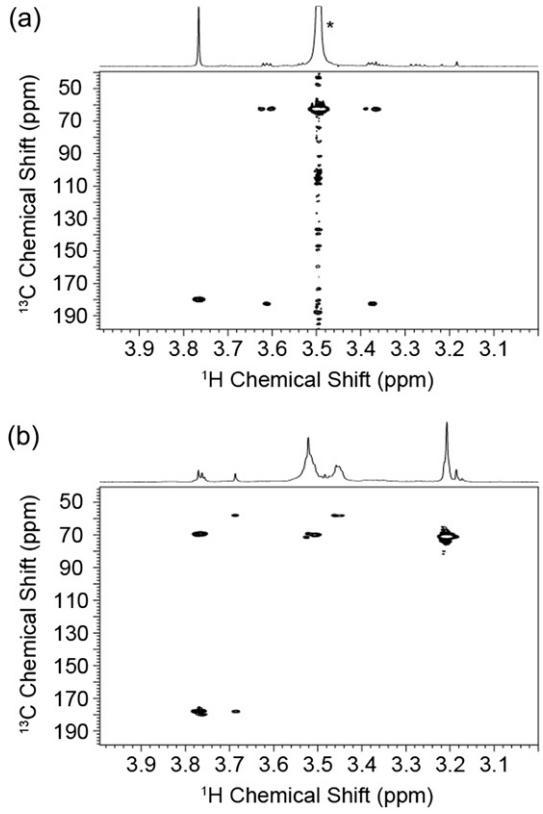

Fig. 5. HMBC (^{1}H–^{13}C) NMR spectra of discharged cathodes (140 mA g^{-1} discharge current density) containing Pd catalyst in (a) 1 M $LiClO_4$ in EC/DMC and (b) 0.3 M $LiClO_4$ in TEGDME. The spectra were collected on a spectrometer with B_0 = 14.1 T (600 MHz), sw = 6134.5 Hz (proton dimension), sw1 = 36199.1 Hz (^{13}C dimension), pw90 = 6 μs, pw90$_x$ = 12.9 μs, at 0.167 s, $d1$ = 1 s and NT = 160 or 544, ni = 256. The spectrum was processed with a 90° shifted sine-bell square window function in VnmrJ 2.1B.

appear in ^{6}Li MAS NMR spectra as a separate peak located in a similar position to LiOH [44].

The lithium powders, depicted in Fig. 1, have similar linewidths with the exception of lithium peroxide. In solid-state NMR, several factors contribute to linewidth including molecular orientations and structural order (short and long-range). The broader linewidth of Li_2O_2 has been seen previously [37,38], and has been attributed to short-range order within the powder and also to the two different charges present on the Li atoms, which slightly affect the chemical shift of each Li nucleus, as described for the Föppl structure of Li_2O_2. The Föppl structure of Li_2O_2 has been suggested to be the most likely structure for lithium peroxide thus far [45–49]. The line broadening of the Li_2O_2 peak in Fig. 2 [38], is most likely due to the same underlying phenomenon as has been described previously [47], as well as short range order effects [47].

The chemical shifts of the discharged cathodes and lithium powders acquired at 7.1 T (not shown) and 17.6 T (Fig. 3a) have similar values, consistent with the trend observed with the powders. Again, this is expected since the quadrupolar coupling constant of ^{6}Li is very small and its behavior is much like that of a spin − 1/2 nucleus. Sample handling and processing were also found to change the observed chemical shifts only slightly. For example, samples maintained in the glove box for two weeks following discharge exhibited chemical shifts slightly more negative than those whose spectra were collected immediately after discharge.

This trend of cathodes containing the two different solvents being grouped into certain chemical shift ranges is significant because it indicates that differences in products formed are mainly solvent-dependent rather than dependent upon the type or presence of different catalysts or other factors. Catalysts do cause slight variation in the chemical shift of discharged cathodes, but do not alter the identity of discharge products to the extent that different solvents do.

Comparing the ^{6}Li NMR chemical shifts obtained from the cathodes containing EC/DMC solvent (depicted in Fig. 3a) with the standards reported in Fig. 2, it is clear that the standard with the closest chemical shift is Li_2CO_3. However, the chemical shifts of the discharged cathodes are not an exact match to the chemical shifts of any of the powder standards alone. This inexact match is attributed to discharge product heterogeneity as has been described previously [15,38]. This heterogeneity means that there are products in addition to the dominant species that contribute to the line shape and chemical shift. In particular, by-products from solvent decomposition [15,19] can add to the peak shape and cause the chemical shifts of the cathodes to be slightly different than that of the dominant discharge product. We suggest that the species with a chemical shift that is closest to the one peak observed, which is Li_2CO_3 for the EC/DMC-containing solvent, is the dominant discharge product in this solvent. This conclusion is identical others utilizing both ^{6}Li MAS NMR [37] as well as other NMR [38] and other spectroscopic techniques [15].

For cathodes discharged in TEGDME, the standard powder with the closest chemical shift to those of the discharged cathodes is that of Li_2O_2, and we suggest that this species is the dominant product formed upon discharge in the TEGDME solvent system. In previous studies, conducted on different ether-based solvents (including both linear and cyclic ethers such as tetraglyme, 1,3-dioxolane and 2-methyl-THF) [19], Li_2O_2 was determined to form in Li–O_2 cathodes. Interestingly, the Li_2O_2 was found to form in the largest quantities during the first discharge. In subsequent cycles the electrolyte solvent was found to decompose to a greater extent until no Li_2O_2 was detected (usually by the 5th cycle) [19]. While subsequent cycles (i.e. after the first discharge) were not studied in this report, the result of finding Li_2O_2 during the first discharge in an ether-based solvent is consistent with results obtained here.

Apart from chemical shift information, NMR peak linewidths can also provide information regarding products formed during discharge [38]. In general, the linewidths obtained from discharged cathodes were about a factor of three greater than those found for the lithium powder standards (shown in Fig. 2). This broadening is attributed to the lack of order in the products of the discharged cathodes and the presence of a conductive carbon matrix, as described previously [38]. However, comparing the linewidths of discharged cathodes in different solvents reveals general trends that can be discerned (Fig. 3). In particular, the NMR linewidths found from the EC/DMC discharged cathodes are narrower (1.21 ppm) relative to those found from TEGDME (1.77 ppm). The narrower linewidth is more closely associated with the Li_2CO_3 standard relative to the broader linewidth attendant Li_2O_2 formation [37,38]. We conclude that Li_2CO_3 is the predominant discharge product in discharged Li–O_2 cathodes containing EC/DMC solvent, while Li_2O_2 is the predominant discharge product in cathodes

Table 1
Calculated Gibbs free energy (ΔG_f°) and formal potential (E°) values for various Li–O_2 battery discharge products.

Final product	Reactants	ΔG_f° (kJ mol^{-1})	E° (V)
Li_2O_2	–	−571.12	2.96
Li_2O	–	−561.91	2.91
Li_2CO_3	Li, O_2, CO_2	−1132.19	5.87
Li_2CO_3	Li_2O_2, $C_{(graphite)}$, O_2	−72.42	0.09
Li_2CO_3	Li_2O_2, CO_2	−3730.23	4.83
Li_2CO_3	Li_2O, CO_2	−237.77	1.23

containing TEGDME, as was suggested for other ether-based solvents [19]. Interestingly, the presence of any of the tested catalysts does not seem to significantly change the identity of the major product, although subtle changes in the chemical shifts do suggest that additional material may be present.

4.3. Solution NMR from discharged cathodes

Analysis of the 2D NMR measurements reveals that cathodes discharged in the two solvents evaluated here (EC/DMC and TEGDME) exhibited both similarities and differences in discharge products. Products found to be present in both types of solvent include lithium formate ($LiCO_2H$, ^1H $\delta = 8.28$ ppm), lithium acetate ($LiCO_2CH_3$, ^1H $\delta = 1.74$) and lithium carbonate (Li_2CO_3). We note that there is also a small amount of acetonitrile (^1H $\delta = 1.90$ ppm) present in the ^1H spectra, which is from the acetonitrile used to rinse the cathodes.

Compounds detected with $^1H/^{13}C$ NMR that are exclusively in EC/DMC include products that result in the low-intensity multiplets in Fig. 5a, which have been determined to be lithium ethylene glycol ($LiOCH_2CH_2OLi$, ^1H $\delta = 3.50$ ppm), lithium propylene glycol ($LiOCH_2CH_3CH_2OLi$, ^1H $\delta = 3.71$, 3.38, 3.28 and 0.98 ppm, connected by cross-peaks in HSQC and HMBC experiments to ^{13}C peaks at 66.33 and 67.95 ppm), an asymmetric compound with chemical formula $LiOCH_2CH_2OCO_2CH_2CH_2OCH_3$ (^1H $\delta = 3.61$, 3.53, 3.50, 3.37 and 3.18 ppm, with cross-peaks to a ^{13}C peak at 181.91 ppm), and a compound with the chemical formula $LiOCH_2OCO_2Li$ (^1H $\delta = 3.77$ ppm), depicted in Table S-3a (in Supplementary data).

In NMR spectra of products formed in cathodes with EC/DMC solvent, the very large peak associated with Li ethylene glycol has been previously reported [19] to form through a reaction between the D_2O (NMR solvent) and the original product formed in Li–O_2 cathodes, Li ethyl dicarbonate ($C_2H_4(OCO_2Li)_2$) [19]. Thus, the presence of Li ethylene glycol indicates that these cathodes have formed large quantities of Li ethyl dicarbonate, which then went on to react with D_2O forming Li ethylene glycol. This intense peak dominates the spectra for cathodes in EC/DMC, as can be seen by the residual peaks (i.e. noise) with the same ^1H chemical shift as this large peak. As a consequence, any compounds that are produced in only small quantities are not seen in the spectra with EC/DMC solvent due to the large peak dominating the spectrum. More cross-peaks due to minor species are present in the 2D NMR spectra of cathodes in TEGDME because it does not contain this large, dominating peak.

Compounds detected with $^1H/^{13}C$ NMR that are exclusively in TEGDME include a long polymer with the chemical formula $-[OCH_2OCO_2CH_2CH_2OCO_2CH_2CH_2OCO_2CH_2O]_n-$ (^1H $\delta = 3.78$, 3.77 and 3.20 ppm with ^{13}C peaks at 69.3, 69.1 and 177.9 ppm) and pure TEGDME (^1H $\delta = 3.53$, 3.52, 3.46, 3.22 ppm), as depicted in Table S-3b (in Supplementary data). Of course, TEGDME is expected in the NMR of cathodes discharged in TEGDME. Additionally, longer chains of $-[OCH_2CH_2O]-$ and $-[OCH_2COO]-$ have been previously reported forming in Li–O_2 cathodes in TEGDME due to esterification and polymerization reactions following nucleophilic attack of radical superoxide and oxidative decomposition [15,19], which may be present here as well. It is therefore apparent that cathodes containing EC/DMC solvent produce a greater number of different types of discharge products than those containing TEGDME.

Interestingly, the presence of Pd in the cathodes does not affect the type or amount of discharge products formed to a great extent, as seen in comparisons of ^1H NMR spectra with and without Pd in the two different solvent systems (as depicted in Supplementary data). There are only slight variations in the different product peak intensities. The solvent appears to play a much larger role in dictating the types of products produced than the presence of this catalyst.

In summary, the discharge products that were produced in both EC/DMC and TEGDME were Li formate, Li acetate and lithium carbonate. Major differences in products formed in cathodes containing the two solvents include the fact that cathodes containing EC/DMC exclusively produce large quantities of Li ethyl dicarbonate (seen as Li ethylene glycol in solution NMR spectra for samples in D_2O), Li propylene glycol, $LiOCH_2OCO_2Li$, and $LiOCH_2CH_2O-CO_2CH_2CH_2OCH_3$, while cathodes containing TEGDME exclusively produce the polymer $-[OCH_2OCO_2CH_2CH_2OCO_2CH_2CH_2O-CO_2CH_2O]_n-$ and additionally contain residual TEGDME. No residual EC/DMC peaks are seen in NMR spectra of cathodes in EC/DMC. Additionally, comparison of the ^1H NMR spectra of cathodes discharged in EC/DMC solvent versus those discharged in TEGDME reveals that cathodes containing EC/DMC produced more solvent decomposition by-products.

5. Conclusions

^6Li MAS NMR spectroscopy has been demonstrated to be a useful tool for the identification of discharge products in Li–O_2 battery cathodes. Major differences in the chemical shifts of discharged cathodes in the two different solvents (EC/DMC and TEGDME) revealed that the primary discharge products of the two solvent systems are different (Li_2CO_3 and Li_2O_2, respectively), which agrees well with previous reports [15,19,38]. Linewidth considerations also indicated this same result. Additionally, minor changes in ^6Li MAS NMR chemical shifts of discharged cathodes containing different catalysts (carbon with Pd or α-MnO_2) indicate that there are slight differences in the types or amounts of discharge products produced with different catalysts.

^{13}C MAS, ^1H and ^{13}C solution NMR spectroscopy confirmed that there are slight variations in the concentrations of different discharge products depending on the type of catalyst used. Additionally, 2D NMR experiments allowed for the identification of by-products formed in the discharged cathodes, theoretically from decomposition of the solvents. The presence of small amounts of these additional by-products account for the slight differences in ^6Li NMR chemical shifts of discharged cathodes compared with lithium powder standards. All of the discharged cathodes containing the two different solvents (EC/DMC and TEGDME) were found to produce lithium formate, lithium acetate and lithium carbonate, and likely also produce CO_2 and H_2O as reported in previous studies [15,19]. Major differences in discharge products found for the two solvents are that cathodes containing EC/DMC produce Li ethyl dicarbonate (seen as Li ethylene glycol in solution NMR spectra of samples in D_2O, which is formed due to a reaction between the original Li ethyl dicarbonate and D_2O), lithium propylene glycol ($LiOCH_2CH_3CH_2OLi$), an asymmetric compound with chemical formula $LiOCH_2CH_2OCO_2CH_2CH_2OCH_3$, and a compound with the chemical formula $LiOCH_2OCO_2Li$. Cathodes containing TEGDME exclusively produce a long polymer with the chemical formula $-[OCH_2OCO_2CH_2CH_2OCO_2CH_2CH_2OCO_2CH_2O]_n-$ and residual TEGDME is also observed in these samples.

Additionally, comparison of the ^1H NMR spectra of cathodes discharged in EC/DMC versus those discharged in TEGDME reveals that cathodes containing EC/DMC produced more solvent decomposition by-products. Two-dimensional correlation NMR spectroscopy (including HSQC, HMBC, COSY and TOSCY experiments) has been found to be a useful tool to investigate by-products formed by decomposition. ^6Li MAS NMR and solution 2D NMR have been found to be highly useful, complementary techniques for the investigation of discharge products in Li–O_2 battery cathodes.

Acknowledgments

This work was supported as part of the Center for Electrical Energy Storage: Tailored Interfaces, an Energy Frontier Research Center funded by the U.S. Department of Energy, Office of Science, Office of Basic Energy Sciences. We also acknowledge Lynn Trahey (Argonne National Laboratory) and Chris Barile (University of Illinois at Urbana-Champaign) for helpful discussions.

Appendix A. Supplementary data

Supplementary data associated with this article can be found in the online version, at http://dx.doi.org/10.1016/j.jpowsour.2013.01.158.

References

[1] K.M. Abraham, Z. Jiang, Journal of The Electrochemical Society 143 (1) (1996) 1–5.
[2] P.G. Bruce, et al., Nature Materials 11 (1) (2012) 19–29.
[3] D. Capsoni, et al., Journal of Power Sources 220 (0) (2012) 253–263.
[4] Z. Peng, et al., Science 337 (6094) (2012) 563–566.
[5] J. Christensen, et al., Journal of The Electrochemical Society 159 (2) (2012) R1–R30.
[6] B.D. McCloskey, et al., The Journal of Physical Chemistry Letters 2 (10) (2011) 1161–1166.
[7] C. Laoire, et al., Journal of The Electrochemical Society 158 (3) (2011) A302–A308.
[8] Y.-C. Lu, et al., Electrochemical and Solid-State Letters 13 (6) (2010) A69–A72.
[9] M.W.J. Chase (Ed.), NIST-JANAF Thermochemical Tables, vol. 9, fourth ed., in: American Institute of Physics, 1998, p. 1510.
[10] M.W.J. Chase (Ed.), NIST-JANAF Thermochemical Tables, vol. 9, fourth ed., in: American Institute of Physics, 1998, p. 1506.
[11] G. Girishkumar, et al., The Journal of Physical Chemistry Letters 1 (14) (2010) 2193–2203.
[12] T. Ogasawara, et al., Journal of the American Chemical Society 128 (4) (2006) 1390–1393.
[13] J. Read, Journal of The Electrochemical Society 149 (9) (2002) A1190–A1195.
[14] J. Read, et al., Journal of The Electrochemical Society 150 (10) (2003) A1351–A1356.
[15] S.A. Freunberger, et al., Journal of the American Chemical Society 133 (20) (2011) 8040–8047.
[16] V.S. Bryantsev, M. Blanco, The Journal of Physical Chemistry Letters 2 (5) (2011) 379–383.
[17] W. Xu, et al., Journal of Power Sources 196 (8) (2011) 3894–3899.
[18] H.-G. Jung, et al., Nature Chemistry 4 (7) (2012) 579–585.
[19] S.A. Freunberger, et al., Angewandte Chemie International Edition 50 (37) (2011) 8609–8613.
[20] B.D. McCloskey, et al., The Journal of Physical Chemistry Letters (2012) 997–1001.
[21] Y.-C. Lu, et al., Journal of the American Chemical Society 132 (35) (2010) 12170–12171.
[22] J.-L. Shui, et al., Journal of the American Chemical Society 134 (40) (2012) 16654–16661.
[23] A. Débart, et al., Angewandte Chemie International Edition 47 (24) (2008) 4521–4524.
[24] L. Trahey, et al., Electrochemical and Solid-State Letters 14 (5) (2011) A64–A66.
[25] H. Wang, et al., Energy & Environmental Science 5 (7) (2012) 7931–7935.
[26] S.H. Oh, L.F. Nazar, Advanced Energy Materials 2 (7) (2012) 903–910.
[27] L. Wang, et al., Journal of The Electrochemical Society 158 (12) (2011) A1379–A1382.
[28] T. Nissinen, et al., Materials Research Bulletin 39 (9) (2004) 1195–1208.
[29] G. Wu, et al., Journal of Solid State Chemistry 177 (10) (2004) 3682–3692.
[30] Y. Wang, H. Zhou, Journal of Power Sources 195 (1) (2010) 358–361.
[31] B. Lu, et al., International Journal of Hydrogen Energy 36 (1) (2011) 72–78.
[32] H.S. Gutowsky, G.E. Pake, The Journal of Chemical Physics 18 (2) (1950) 162–170.
[33] E.R. Andrew, A. Bradbury, R.G. Eades, Nature 182 (4650) (1958) 1659.
[34] Z. Xu, J.F. Stebbins, Solid State Nuclear Magnetic Resonance 5 (1) (1995) 103–112.
[35] C.P. Grey, N. Dupré, Chemical Reviews 104 (10) (2004) 4493–4512.
[36] H. Günther, et al., Angewandte Chemie International Edition in English 26 (12) (1987) 1212–1220.
[37] J. Xiao, et al., Journal of Power Sources 196 (13) (2011) 5674–5678.
[38] M. Leskes, et al., Angewandte Chemie International Edition 51 (34) (2012) 8560–8563.
[39] J.-K. Lee, et al., Chemistry of Materials 21 (1) (2008) 6–8.
[40] D. Guyomard, J.M. Tarascon, Journal of The Electrochemical Society 139 (4) (1992) 937–948.
[41] N.E. Jacobsen, NMR Spectroscopy Explained: Simplified Theory, Applications and Examples for Organic Chemistry and Structural Biology, Wiley-Interscience, Hoboken, NJ, 2007.
[42] B.D. McCloskey, et al., Journal of the American Chemical Society 133 (45) (2011) 18038–18041.
[43] Y.-C. Lu, et al., Energy & Environmental Science 4 (8) (2011) 2999–3007.
[44] J.Z. Hu, et al., Journal of Power Sources 182 (1) (2008) 278–283.
[45] F. Fehér, I. Von Wilucki, G. Dost, Chemische Berichte 86 (11) (1953) 1429–1437.
[46] H. Föppl, Zeitschrift für anorganische und allgemeine Chemie 291 (1–4) (1957) 12–50.
[47] M.K.Y. Chan, et al., The Journal of Physical Chemistry Letters 2 (19) (2011) 2483–2486.
[48] L.G. Cota, P. de la Mora, Acta Crystallographica Section B 61 (2) (2005) 133–136.
[49] M.D. Radin, et al., Journal of the American Chemical Society 134 (2) (2011) 1093–1103.